# Copper/Nickel/Manganese Doped Cerium Oxides Based Catalysts for Hydrogenation of CO₂

**Susilawati Toemen, Wan Azelee Wan Abu Bakar,[*] and Rusmidah Ali**

*Department of Chemistry, Faculty of Science, Universiti Teknologi Malaysia, 81310 Skudai, Johor Malaysia*
*[*]E-mail: wanazelee@yahoo.com*

The recycling technology by the catalytic conversion is one of the most promising techniques for the $CO_2$ treatment of coal burning power plant flue gases. The conversion of $CO_2$ to valuable product of $CH_4$ can be used as a fuel to run the turbine for electricity generation. Through this technique, the amount of coal needed for the combustion in a gas turbine can be reduced as well as $CO_2$ emissions. Therefore, a series of catalysts based on cerium oxide doped with copper, nickel and manganese were prepared by impregnation method. From the characterization analysis, it showed that the prepared catalysts calcined at 400 ℃ were amorphous in structure with small particle size in the range below 100 nm. Meanwhile, the catalyst particles were aggregated and agglomerated with higher surface area of 286.70 $m^2g^{-1}$. By increasing the calcination temperature of catalysts to 1000 ℃, the particle sizes were getting bigger (> 100 nm) and having moderate crystallinity with lower surface area (67.90 $m^2g^{-1}$). From the catalytic testing among all the prepared catalysts, Mn/Ce-75/$Al_2O_3$ calcined at 400 ℃ was assigned as the most potential catalyst which gave 49.05% and 56.79% $CO_2$ conversion at reaction temperature of 100 ℃ and 200 ℃, respectively.

**Key Words :** Carbon dioxide, Catalyst, Hydrogenation, Coal burning power plant, Flue gas

## Introduction

According to United Nations Development Report (2007), Malaysia ranked as the 26th largest greenhouse gases emitters with the population over 27 million people.[1] The major contributor of greenhouse gases is from power plant since, the chemical composition of Mnajung Coal Burning Power Plant (Perak, Malaysia) flue gases contained mainly of carbon dioxide and water vapour. This showed that removing $CO_2$ gases from that type of plant is very important for maintaining a green environment. Therefore, the recycling technology by the catalytic conversion is one of the most promising techniques for the $CO_2$ treatment of coal burning power plant flue gases since the production of $CH_4$ can also be used as a fuel to run turbine for electricity. By recycling the $CO_2$ *via* this technique, the amount of coal needed for the combustion in a gas turbine can be reduced as well as $CO_2$ emissions. In order for this method to be effective, the production of catalysts and its behaviour should be investigated further.

The current technologies that has been investigated by many researchers for the treatment of carbon dioxide in coal burning power plant flue gases is Integrated Gasification Combined Cycle (IGCC) which involved high maintenance fees which is not cost effective.[1] In fact, there is no method applied to remove $CO_2$ in coal power plant flue gases and also there is no research done that used catalyst under this condition. Thus, a new technology that is the catalytic conversion method made from cerium oxide, $CeO_2$ catalyst will be introduced in this research.

Cerium oxide was usually used as a catalyst in industry for various types of reactions including solid state chemistry, biotechnology, organic reactions and environmental management. The $NO_2$ and $SO_2$ reduction reactions are also catalyzed by cerium oxide.[3,4] Thus, the cerium oxide is effective material for $CO_2$ methanation in coal burning power plant since flue gases from that type of plant consists of $NO_2$ and $SO_2$. The catalysts containing cerium oxide will resist and stable without deactivated by these gases. In addition, a highly basic catalyst such as $CeO_2$ is proposed to enhance carbon dioxide adsorption and chemisorptions on the catalyst surface. It has excellent redox properties owing to the very fast reduction of $Ce^{4+}/Ce^{3+}$, which is associated with the formation of oxygen vacancies at the surface.[5]

However, the $CeO_2$ is seldom used alone because a high degree of textural stability of $CeO_2$ catalyst can only be obtained by doping or modifying the preparation parameters.[6] Therefore, $CeO_2$ is often combined with other metal oxides generally from active transition and noble metals. The addition of Ni as a second metal in this research is the best method to promote the formation of methane since nickel was categorized as active material for methanation of carbon dioxide due to their high catalytic activity and high selectivity to methane.[7]

Therefore, this research is looking at ways to convert carbon dioxide to higher value added product of $CH_4$ by using cerium based catalyst which could provide means for sustainable development. For that reason, it is necessary to remove the carbon dioxide from the flue gas of coal burning power plant *via* chemical conversion technique. This process is not only creates a green and sustainable environment but produces the methane gas which can also be used as a fuel to

run turbine for electricity. In order for this method to be effective, a suitable catalyst should be prepared that has higher basicity and higher surface area with small particle size which is highly dispersed on the catalyst surface. Such characteristic must be applied to promote the selective $CO_2$ methanation gas process by reduction reaction.

## Experimental

**Preparation of Catalysts.** All the catalysts were prepared by aqueous incipient wetness impregnation method. 5 g of $Ce(NO_3)_2 \cdot 2H_2O$ obtained from MERCK was dissolved in small amount of distilled water. Mixed catalyst solution was prepared by mixing an appropriate amount of second metal which were 2.05 g of Cu, 2.46 g of Mn or 2.66 g of Ni nitrate salts (Sigma Aldrich) with $Ce(NO_3)_2 \cdot 2H_2O$ solution according to its ratio listed in Table 1. A homogeneous mixture was obtained by electromagnetic stirring at room temperature for 30 minutes. Alumina beads with diameter of 3 mm were used as support material in this study. The support was immersed into the catalysts solution until the solution was evenly absorbed on the surface of the support. The coating process was repeated three times with drying at ambient temperature for every coating process. It was then aged inside an oven at 80–90 °C for 24 h followed by calcinations using a furnace in the air atmosphere at 400 °C for 5 h using a ramp rate of 10 °C/min to remove all the metal counter ions and water present in the catalyst.

**Characterization.** The prepared catalyst undergoes several characterization techniques to study its chemical and physical properties. The structure of the catalyst was determined by X-ray Diffraction (XRD) using Cu Kα radiation ($\lambda = 1.54060$ Å). Data was collected over the range of 2θ from 20° to 80° and analyzed by a PC interfaced to the diffractometer using software called Diffrac Plus. Field Emission Scanning Electron Microscopy analysis was measured using a Ziess Supra 35VP FESEM with the energy of 15.0 kV couple with EDX analyzer in order to determine the morphology and elemental composition of the catalyst. The sample was bombarded using an electron gun with a tungsten filament under 25 kV resolution to get the required magnification image. $N_2$ adsorption/desorption isotherm analysis of the catalyst was obtained using Micromeritics ASAP 2010 volumetric adsorption analyzer at −196 °C. Prior to the measurement, the calcined catalysts were degassed at 120 °C overnight. The isotherms were used to determine the following parameters: surface area [using Brunauer–Emmett–Teller (BET) equation], total pore volume, total micropore volume, and total mesopore volume. Temperature Programmed Reduction (TPR) was carried out with pure hydrogen gas inside a Shidmadzu TGA-50 analyzer. About 30-40 mg of sample was heated from room temperature to 1000 °C at a heat ramp rate of 3 °C/min. The hydrogen flow rate for all experiments was 200 mL/min.

**Catalytic Activity Measurement.** The catalytic $CO_2$ methanation reaction was performed under atmospheric pressure in a fixed microreactor and analyzed *via* online FTIR

Nicolet Avatar 670 DGTS. The 10 g of supported catalyst was placed in the middle of the glass tube made of Pyrex glass with diameter 10 mm and length of 520 mm. It was then secure with glass wool at both ends. The reaction gas mixture (inlet) consisting of $CO_2$, $H_2$, $N_2$, $O_2$ (10/40/39/11 mL/min) was passed continuously through the catalyst and was heated in an isothermal tube furnace. The total flow rate was set to 100 mL/min while, the weight hourly space velocity was kept fixed at 636 mLg$^{-1}$ h$^{-1}$. The feed gas flow rate was adjusted with a mass flow controller and the reaction temperature was performed from 60 °C up to 300 °C with the increment temperature rate of 5 °C/min. Off line GC analysis was done to determine the yield of $CH_4$ gas due to the low sensitivity of FTIR spectroscopy towards the stretching band of $CH_4$. The Hewlett Packard 6890 Series Gas Chromatography System with capillary column (Brand: Ultra 1 932530) with 25.0 m × 200 μm × 0.11 μm nominal column was used in this research. The initial temperature was 40 °C for 7 minutes and the injection temperature was 150 °C. The detection temperature for this analysis was 300 °C. The component present in outlet stream from the column was detected by Flame Ionization Detector (FID) after the analysis was completed. Before the analysis, calibration of methane was carried out using internal standard 99% pure methane gas. The concentration of methane produced by the catalytic testing was calculated by referring to the peak area of samples chromatogram and the standard methane graph.

## Results and Discussion

**Characterization.** In this research, the loading of cerium was fixed to 75 wt % while, the second metal was 25 wt %. This content was confirmed by Energy Dispersive X-ray (EDX) analysis and is summarized in Table 1. The result was taken before the catalyst was calcined at 400 °C for 5 h. It can be seen that the ratio obtained from the EDX analysis was almost an equal value as stated in the catalyst ratio.

Meanwhile, the BET surface area and pore diameter of the prepared catalyst with different calcination temperature are also listed in Table 1. All the catalysts calcined at 400 °C displayed a higher surface area with smaller pore diameter. However, the physicochemical properties of each catalyst were slightly different depending on the identity of the second metal. It clearly showed that by incorporating Cu to the $Ce/Al_2O_3$ (210.42 m$^2$g$^{-1}$) catalyst, a lower surface area about 200.82 m$^2$g$^{-1}$ was obtained. It is possibly due to the pore blocking by the promoter that had occurred during impregnation step as suggested by Seo *et al.*[8] Compared with Cu/Ce-75/Al$_2$O$_3$ catalyst, the catalyst promoted by nickel showed slightly higher surface area which was 205.15 m$^2$g$^{-1}$ might be due to the different spreading of active Ni on $Al_2O_3$ support.

Nonetheless, Mn/Ce-75/Al$_2$O$_3$ (a) catalyst calcined at 400 °C had shown the highest surface area (286.70 m$^2$g$^{-1}$) among the three dopants that were used in this research. This result indicates that the addition of Mn towards cerium catalyst leads to the production of new active sites and hence

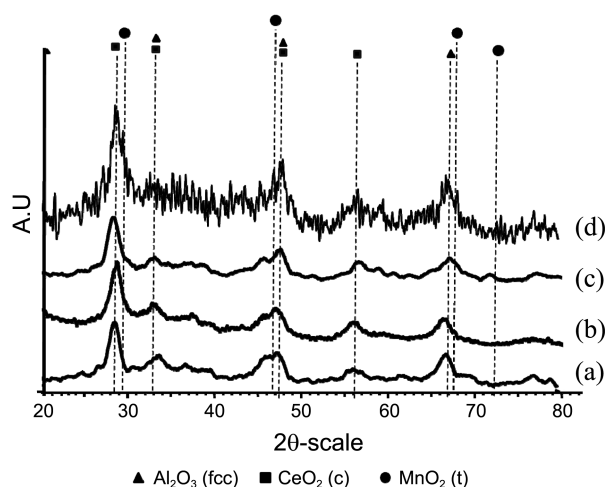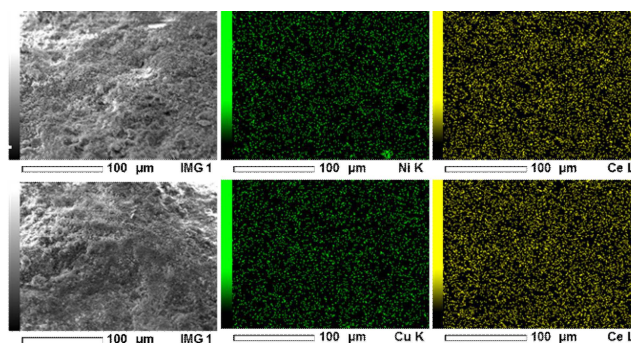**Table 1.** Cerium based catalysts prepared by wetness impregnation method

| Catalyst | Calc. Temp ($^o$C) | Weight loading (wt %) | | | | BET Surface Area (m$^2$/g) | Average Pore Diameter (nm) | Cryst. Size (nm)[a] |
|---|---|---|---|---|---|---|---|---|
| | | Ce | Cu | Ni | Mn | | | |
| Ce-100/Al$_2$O$_3$ | 400 | 12.63 | – | – | – | 210.42 | – | 11.44 |
| Cu/Ce-75/Al$_2$O$_3$ | 400 | 13.41 | 5.37 | – | – | 197.04 | – | 35.56 |
| Ni/Ce-75/Al$_2$O$_3$ | 400 | 12.99 | – | 5.42 | – | 205.15 | 7.493 | 24.14 |
| Mn/Ce-65/Al$_2$O$_3$ | 400 | 11.34 | – | – | 5.43 | 200.82 | – | 29.69 |
| Mn/Ce-75/Al$_2$O$_3$ (a) | 400 | 11.68 | – | – | 5.26 | 286.70 | 6.654 | 19.24 |
| Mn/Ce-75/Al$_2$O$_3$ (b) | 1000 | 15.86 | – | – | 2.78 | 67.90 | – | 57.05 |
| Mn/Ce-85/Al$_2$O$_3$ | 400 | 15.04 | – | – | 1.86 | 195.43 | – | – |

[a]Crystallite size calculated by Scherer Equation XRD.

increases its surface area. Lowering the cerium content to 65 wt % over Mn/Ce-65/Al$_2$O$_3$ catalyst, the surface area became lowered to 200.82 m$^2$g$^{-1}$. Similar result occurs to the catalyst with cerium content of 85 wt %. The surface area of Mn/Ce-85/Al$_2$O$_3$ catalyst only achieved 195.43 m$^2$g$^{-1}$. From these results, it showed that 75 wt % of Ce loading was the best to have higher BET surface area.

Furthermore, the XRD pattern of Ce-100/Al$_2$O$_3$, Cu/Ce-75/Al$_2$O$_3$, Ni/Ce-75/Al$_2$O$_3$ and Mn/Ce-75/Al$_2$O$_3$ catalysts that were calcined at 400 $^o$C (Figure 1) showed very low degree of crystallinity and high noise to signal ratio. The peaks assigned to the face centre cubic (fcc) Al$_2$O$_3$ was appeared at 2θ = 33.545, 47.535 and 66.865$^o$. It is noteworthy that the peaks of cubic CeO$_2$ exhibit obvious reflection at 28.680$^o$ and 56.341$^o$. Another two peaks of CeO$_2$ were observed in the broad shoulder of alumina support at 2θ = 33.545 and 47.535$^o$. No peaks for NiO and CuO crystalline phases could be detected in the diffractograms of Cu/Ce-75/Al$_2$O$_3$ (Figure 1(b)) and Ni/Ce-75/Al$_2$O$_3$ (Figure 1(c)) catalysts. This suggested that NiO and CuO have smaller particles size with highly dispersed on the catalyst surface (Figure 2) which was under the detection limit of XRD measurements.

Interestingly, the tetragonal MnO$_2$ peaks were found at 2θ = 29.281, 46.082, 67.556 and 72.384$^o$ over Mn/Ce-75/Al$_2$O$_3$



**Figure 2.** EDX Mapping profile over Ni/Ce-75/Al$_2$O$_3$ and Cu/Ce-75/Al$_2$O$_3$ catalysts calcined at 400 $^o$C for 5 h.

catalyst (Figure 1(d)) even calcined at 400 $^o$C. The intensity of these peaks became increased and intensed especially at 2θ = 29.281 after cerium loading decreased to 65% (Figure 3(a)). It is because Mn content is higher over Mn/Ce-65/Al$_2$O$_3$ catalyst as obtained in EDX analysis in Table 1.



**Figure 1.** XRD diffractograms of (a) Ce-100/Al$_2$O$_3$ (b) Cu/Ce-75/Al$_2$O$_3$ (c) Ni/Ce-75/Al$_2$O$_3$ (d) Mn/Ce-75/Al$_2$O$_3$ catalysts calcined at 400 $^o$C.

▲ Al$_2$O$_3$ (fcc)   ■ CeO$_2$ (c)   ● MnO$_2$ (t)
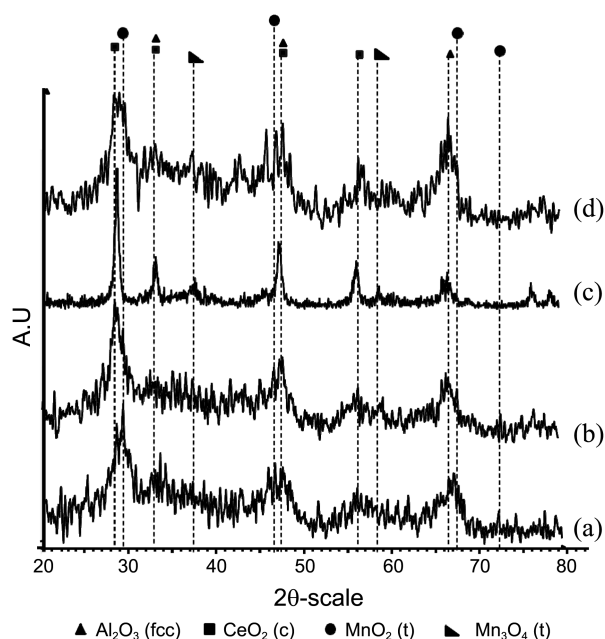


**Figure 3.** XRD diffractograms of a) Mn/Ce-65/Al$_2$O$_3$, b) Mn/Ce-75/Al$_2$O$_3$ (a), c) Mn/Ce-75/Al$_2$O$_3$ (b) and d) Mn/Ce-85/Al$_2$O$_3$ catalysts.

▲ Al$_2$O$_3$ (fcc)   ■ CeO$_2$ (c)   ● MnO$_2$ (t)   ◣ Mn$_3$O$_4$ (t)

However, the broad peak was observed at similar location over catalyst with Mn loading of 85 wt % because of the overlapping of $MnO_2$ with $CeO_2$ peaks. When approaching towards the higher calcination temperature of 1000 °C, the Mn/Ce-75/$Al_2O_3$ catalyst turns to be in high crystallinity (Figure 3(c)). As expected, the tetragonal $MnO_2$ species that was observed at calcination temperature of 400 °C had transformed to tetragonal $Mn_3O_4$. The two peaks regarding this species was found at $2\theta = 37.129°$ ($I_{100}$) and 58.164° ($I_{50}$).

Similar peaks of cubic $Al_2O_3$ and $CeO_2$ compounds become more apparent and profound at their respective location. This phenomenon automatically decreases its surface area around 75% after the catalyst was calcined at 1000 °C as shown in Table 1. A drastic decrease in surface area on increasing the calcination temperature was obviously due to the particle enlargement from sintering that occurred during calcination process. However, the average particles size of the catalyst is not more than 60 nm and it still categorized as nano particles size. This was proven by FWHM data in Table 1.

The TPR profiles of Mn/Ce/$Al_2O_3$ catalysts are shown in Figure 4. The reduction of each Ce and Mn oxides species to its lower oxidation number are observed. The lower reduction temperature shoulder peak of the Mn/Ce-75/$Al_2O_3$ (a) catalysts calcined at 400 °C was located at 270 °C related to the reduction of $MnO_2$ to $Mn_2O_3$. The broader TPR peaks from 400 °C to 500 °C is then can be assigned to the overlapping peaks between the reduction of $Mn_2O_3$ to $Mn_3O_4$ and $CeO_2$ to $Ce_2O_3$. The last reduction step which converted $Mn_3O_4$ to MnO, occurred at 850 °C.

By increasing the calcination temperature to 1000 °C, the first and second reduction peaks of Mn/Ce-75/$Al_2O_3$ (b) were shifted to a higher reduction temperature. The intensity for first reduction peak (300-450 °C) becomes smaller while, higher for second reduction peak (690 °C). These results indicate that the primary Mn species occurred over Mn/Ce-75/$Al_2O_3$ catalyst calcined at 1000 °C was initially $Mn^{3+}$. It was in align with the results obtained by Lee *et al.*[9] who
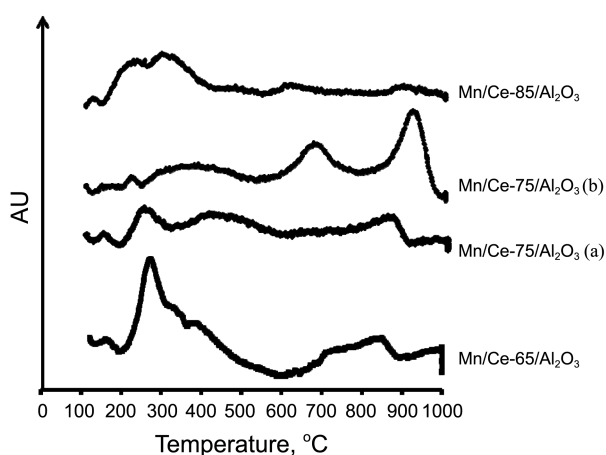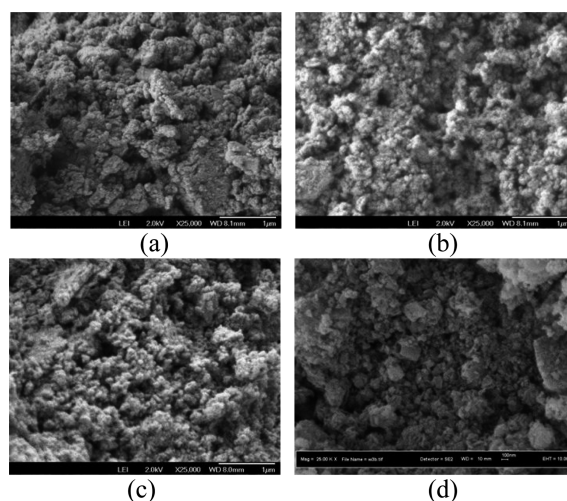


**Figure 5.** FESEM micrographs of fresh (a) Ce-100/$Al_2O_3$, (b) Cu/Ce-75/$Al_2O_3$ (c) Ni/Ce-75/$Al_2O_3$, (d) Mn/Ce-75/$Al_2O_3$ calcined at 400 °C for 5 h with magnification 25000X.

found that the reduction peak of $MnO_2$ to $Mn_2O_3$ was not observed at all in their Mn/$TiO_2$ catalysts calcined above 600 °C. The higher reduction peak of $Mn_3O_4$ to MnO was then observed at temperature above 900 °C. As reported by Peña *et al.*,[10] the higher reduction temperatures were required for the catalysts that were calcined at higher temperatures. It was due to the stronger metal-support interactions which could not easily be reduced.

Furthermore, the reduction profile of Mn/Ce/$Al_2O_3$ catalyst calcined at 400 °C change significantly as the cerium loading decreases to 65 wt %. It can be seen that the intensity of the first reduction peak at 270 °C over Mn/Ce-65/$Al_2O_3$ catalyst was higher indicating that the larger amount of $Mn^{4+}$ species was reduced. It is because the Mn content over this catalyst is higher compared to the other catalysts as proven in EDX (Table 1) and XRD analysis (Figure 3(a)). Meanwhile, the Mn/Ce-85/$Al_2O_3$ catalyst gives only two reduction peaks with maximum at 300 °C.

FESEM images of the Ce-100/$Al_2O_3$, Cu/Ce-75/$Al_2O_3$, Ni/Ce-75/$Al_2O_3$, Mn/Ce-75/$Al_2O_3$ catalysts calcined at 400 °C are shown in Figure 5. It clearly shows that the catalyst particles over prepared catalysts were aggregated and agglomerated each other on the surface of the catalyst to form rough surface morphology. However, it can be seen that the catalyst having smaller particle size with many pores formed which plays an important role to exhibit the higher catalytic activity. The pores of the catalyst will provide the space for the access of active metal components to attract $CO_2$ and $H_2$ molecules on the catalyst surface. These results are consistent with the results of FWHM from XRD analysis which revealed the nano particle sizes for each catalyst. Thus, a very broad peak denoting an amorphous state was observed in the diffratogram calcined at 400 °C caused by the very small nanocrystallites size.

The morphology of Mn/Ce-75/$Al_2O_3$ catalyst has changed significantly after decreasing and increasing the Ce loading (Figure 6). It showed that the agglomerated particles became
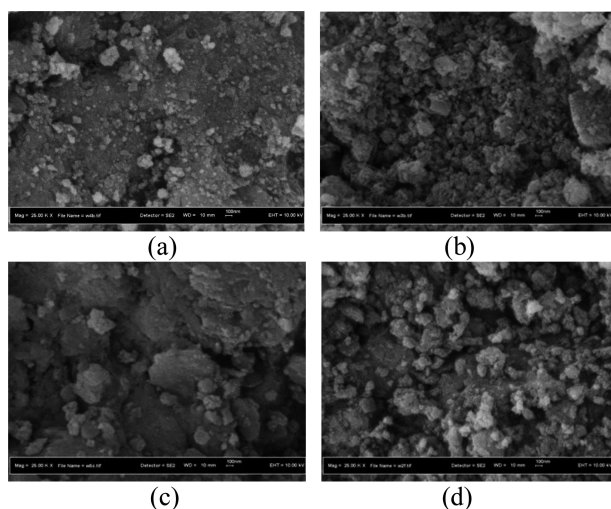


**Figure 4.** TPR profiles of Mn/Ce/$Al_2O_3$ at different loading and different calcination temperatures.

**Figure 6.** FESEM micrographs of fresh (a) Mn/Ce-65/Al₂O₃, (b) Mn/Ce-75/Al₂O₃ (c) Mn/Ce-85/Al₂O₃ catalysts calcined at 400 ᵒC and (d) Mn/Ce-75/Al₂O₃ calcined at 1000 ᵒC for 5 h with magnification 25000X.

densely packed on the catalyst surface until there is no sphere shape observed. However, after the catalyst was subjected to higher calcination temperature of 1000 °C, the larger agglomerated particles in irregular size was observed. This result is in line with the XRD analysis which revealed the sharp and intense peaks denoting to the high crystallinity phase thus, decreasing its surface area. Based on the characterization results, it is expected that Mn/Ce-75/Al₂O₃ catalysts calcined at 400 ᵒC would show a high catalytic activity in the $CO_2$ methanation reaction.

**Catalytic Performance.**

**Effect of Promoter:** The performance of the alumina supported cerium based catalysts calcined at 400 ᵒC for 5 h were tested in a fixed bed microreactor coupled with FTIR. The $CO_2$ conversion of the ceria based catalysts is shown in Figure 7 and methane production in Table 2. It can be seen that the initial activity of Ce/Al₂O₃ catalyst gives only 1.44% at reaction temperature of 100 ᵒC and increased to 7.39% conversion of $CO_2$ at higher reaction temperature of 300 ᵒC.

As expected, Ni/Ce-75/Al₂O₃ catalyst was considerably more active than Cu/Ce-75/Al₂O₃ and managed to convert around 35.24%, 43.09% and 45.94% at reaction temperature
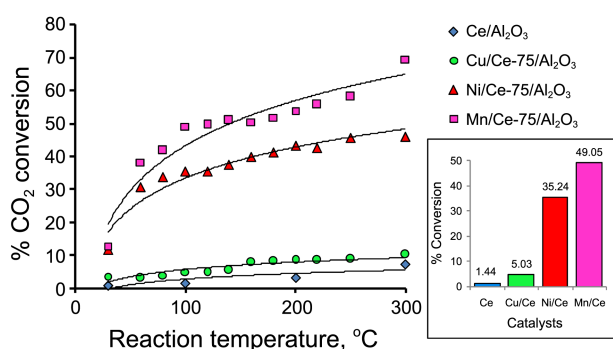


**Figure 7.** Catalytic performance of $CO_2$ methanation reaction over various alumina supported cerium oxide based catalysts.

**Table 2.** The methane product detected *via* GC over alumina supported cerium oxide based catalysts calcined at 400 ᵒC for 5 h

| Catalyst | Methane Production (%) | | | TOF[a] ($10^{-2}$ S⁻¹) | S[b] (%) |
|---|---|---|---|---|---|
| | 100 ᵒC | 200 ᵒC | 300 ᵒC | | |
| Ce (100)/Al₂O₃ | – | – | 0.92 | 0.10 | 12.45 |
| Cu/Ce-75/Al₂O₃ | – | – | 2.78 | 0.17 | 21.04 |
| Ni/Ce-75/Al₂O₃ | 0.06 | 1.48 | 5.19 | 0.42 | 17.68 |
| Mn/Ce-75/Al₂O₃ | 0.22 | 8.12 | 27.35 | 1.04 | 39.39 |

[a]Turnover frequency (TOF) value at reaction temperature of 300 ᵒC.
[b]Selectivity at reaction temperature of 300 ᵒC

of 100 ᵒC, 200 ᵒC and 300 ᵒC, respectively. The catalyst yielded 5.19% of methane at maximum reaction temperature. On the contrary, the $CO_2$ conversion of Cu/Ce-75/Al₂O₃ catalyst only gave 10.23% conversion with methane production of 2.15% at reaction temperature of 300 ᵒC. Although, Kosmambetova *et al.*[11] suggest that the interaction between copper oxide and cerium oxide may enhance the redox properties of both components, but it was not enough to give higher catalytic activity compared to Ni/Ce-75/Al₂O₃ catalyst. Besides, the surface area and particles size of Cu/Ce catalyst obtained is lower and bigger than Ni/Ce-75/Al₂O₃ catalyst as stated in Table 1.

The catalytic performance is further improved when manganese was added into Ce/Al₂O₃ catalyst to form Mn/Ce-75/Al₂O₃ catalyst and managed to convert $CO_2$ around 49.05% at 100 ᵒC and 56.79% at 200 ᵒC. The catalyst gave maximum $CO_2$ conversion of 69.44% at maximum reaction temperature of 300 ᵒC with 27.35% of methane. The other 42.09% of $CO_2$ conversion was probably formed the intermediate product of CO. Meanwhile, the Mn/Ce-75/Al₂O₃ catalyst exhibited highest increase in turn over frequency (TOF) as indicated in Table 2.

These show that the Mn is more compatible and active to be added to the cerium based catalyst compared to Ni and Cu. It will greatly improve the surface $Ce^{4+}$ reducibility, gives smaller particles size with larger surface area as suggested by Ocampo *et al.*[12] and Zhang *et al.*[13] The highly dispersed or spreading of Mn crystallites on the catalyst surface will cause the catalyst to have higher surface area as can be seen in Table 1. Overall, the conversion of $CO_2$ towards all the prepared catalysts increased apparently with the increasing of reaction temperature.

**Effect of Calcination Temperatures:** This parameter was studied in order to find out the effect of calcination temperature on alumina supported catalyst towards $CO_2$ conversion. The prepared catalysts were aged first in an oven for 24 h before calcined at 300 ᵒC, 400 ᵒC, 500 ᵒC, 700 ᵒC and 1000 ᵒC. Figure 8 indicates the trend plot of catalytic activity over Mn/Ce-75/Al₂O₃ catalyst at various calcination temperatures.

It clearly shows that the best calcination temperature over Mn/Ce-75/Al₂O₃ catalyst is at 400 ᵒC with 49.05% $CO_2$ conversion at reaction temperature of 100 ᵒC. The catalytic activity of this catalyst was then started to decline to 33.87% when calcination temperature was increased to 500 ᵒC. As
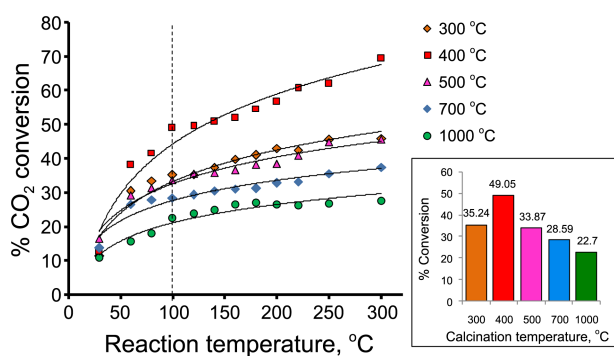
**Figure 8.** Catalytic performance of $CO_2$ conversion from methanation reaction over Mn/Ce-75/$Al_2O_3$ catalyst calcined for 5 h at different calcination temperatures.



**Figure 9.** Catalytic performance of $CO_2$ conversion from methanation reaction over Mn/Ce-75/$Al_2O_3$ catalyst calcined at 400 °C for 5 h with various cerium loading.

the calcination temperature was further increased to 700 °C, the $CO_2$ conversion of Mn/Ce-75/$Al_2O_3$ catalyst was further decreased to 28.59%. Upon the extreme calcination temperature at 1000 °C, the conversion of $CO_2$ gave only 22.70% which decreased more than 50% conversion compared to the catalyst calcined at 400 °C.

Deactivation of these catalysts could be due to the sintering effect that occurred during calcination process. The structural changes of Mn/Ce-75/$Al_2O_3$ catalyst can obviously be observed in XRD analysis in Figures 3(b) and 3(c). The transition from amorphous state (400 °C) to crystalline state (1000 °C) explained the increasing of particles size of the catalyst which is increased around 65%. It is in a good agreement with Oh *et al.*[14] and Ocampo *et al.*[12] who said that the growth in crystallite size and the morphology on the surface of catalysts have strong relationship with the calcination temperatures thus decreasing the surface area consequently produces less active catalyst hence lowered the catalytic activity.[12] Therefore, the larger particles of that catalyst can also be observed in FESEM analysis (Figure 6(d)).

Therefore, 400 °C was the optimum calcination temperature over Mn/Ce-75/$Al_2O_3$ catalyst. In other words, the conversion of $CO_2$ for the catalyst with different calcination temperatures is in the increasing order as follows : 400 °C > 300 °C > 500 °C > 700 °C > 1000 °C. Then, the catalysts were further tested with different cerium loading.

**Effect of Cerium Loading:** The effect of cerium loading was conducted in order to investigate the optimum loading towards the performance of $CO_2$ conversion. Figure 9 shows the detail trend plot of amount cerium loading towards $CO_2$ conversion of Mn/Ce/$Al_2O_3$ catalyst calcined at 400 °C. The cerium loading used were 65 wt %, 70 wt %, 75 wt %, 80 wt % and 85 wt %. It is clear that the loading of cerium had significant influence on the $CO_2$ conversion.

The performance of the Mn/Ce-75/$Al_2O_3$ (a) catalyst calcined at 400 °C was already discussed above. It can convert $CO_2$ around 49.05% at reaction temperature of 100 °C. Lowered the content of cerium to 70 and 65 wt % could also decreased the performance of the catalyst. However, when the loading was increased slightly to 80 wt % (Mn/Ce-80/$Al_2O_3$), the $CO_2$ conversion was reduced to 34.46%. As
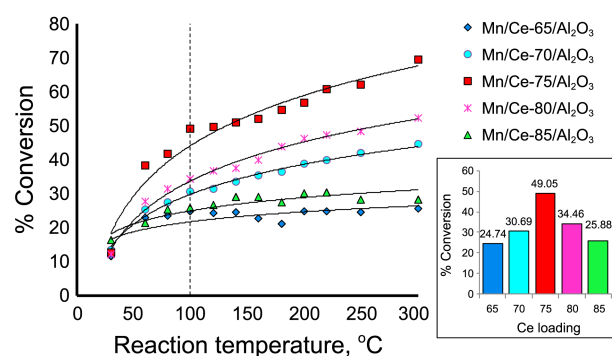
the $CeO_2$ content was increased to 85 wt %, the $CO_2$ conversion was severely dropped to 25.88%. The decreasing activity of this catalyst is possibly due to the coverage effect of $CeO_2$ on the catalyst surface as shown in FESEM analysis in Figure 6(c) which will cause the formation of agglomerate hence decreasing the available active sites.[15,16] The blocking on the catalyst pores structure could also be occurred when highest amount of cerium was used thus decreased the pore volume and size as had been explained by Perkas *et al.*[17] in their Ni-Zr-Ce catalyst. From this observation, it can be concluded that the cerium loading of 75 wt % for Mn/Ce/$Al_2O_3$ catalyst would be the optimum value and follows the trend of activity in the order of 75 wt % > 80 wt % > 70 wt % > 85 wt % > 65 wt %.

From Figure 9, it can be summarized that the activity and selectivity of the catalyst depend strongly on their surface composition and structure.[18] An appropriate amount of Mn and Ce would improve the catalyst activity. The Mn/Ce/$Al_2O_3$ catalyst with the ratio of 25:75 which gave the best catalytic performance was further studied on their effect of pre-treatment.

**Effect of Reduction Pretreatment of Supported Cerium Catalysts:** The effect of reduction pretreatment over Mn/Ce-75/$Al_2O_3$ catalyst is reported in Figure 10. Prior to the start of testing, all the prepared catalysts were underwent air pretreatment at 100 °C for 30 minutes. The reason to preheat the catalyst is to activate the catalyst as well as to remove the
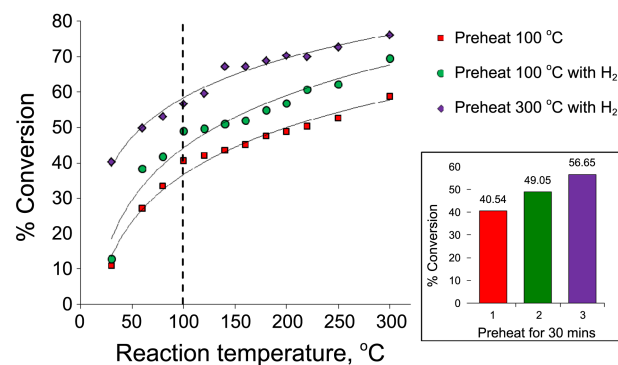


**Figure 10.** Catalytic performances of $CO_2$ conversion from methanation reaction over Mn/Ce-75/$Al_2O_3$(a) catalyst preheat at 100 °C and 300 °C with or without $H_2$ gas for 30 mins before reaction.

moisture in the catalyst. In this research, Mn/Ce-75/Al₂O₃ catalyst also underwent pretreatment in the presence of $H_2$ gas (40 mL/min) at temperature of 100 °C or 300 °C for half an hour which was under reduction condition. As such, the entire active sites on the surface of the catalyst will be reduced to lower oxidation number or to metallic state consequently increased its catalytic activity.

The Mn/Ce-75/Al₂O₃ (a) catalyst that was pretreated with or without flow of $H_2$ gas at 100 °C gave almost similar results which around 49.05% and 40.54% at reaction temperature of 100 °C. However, the performance of catalyst increased to 56.65% at similar reaction temperature after pretreat at 300 °C for 30 minutes with $H_2$ gas. This result shows that the reduction pretreatment will caused the reorganization of the surface structure as claimed by Kim *et al*.[19] in their Ni catalyst. They found that the C-O bond was weakened by the active oxygen on NiO, preferentially reacts with $H_2$ and surface carbon intermediate facilitated by NiO was easily hydrogenated to produce methane. The similar result was reported by Tada *et al*.[20] who had investigated the effect of reduction pretreatment on the activity of CO methanation over Ru/Al₂O₃ catalyst. The 13.5% of CO methanation was achieved from their results at reduction pretreatment temperature of 300 °C and decreased to 6.0% as the temperature was raised to 600 °C.

**Reproducibility Testing:** The reproducibility activity towards Mn/Ce-75/Al₂O₃ catalyst calcined at 400 °C was conducted by using the same catalyst several times. The trend plot of reproducibility testing over this catalyst is shown in Figure 11. For the first testing, the catalyst was preheated at 300 °C for 30 mins in the presence of $H_2$. After that, no pretreatment was conducted for the next testing.

It can be seen that the conversion of CO₂ over this catalyst for the first test was 70.28% at reaction temperature of 200 °C. However, the conversion was decreased to 44.27% after second testing using the similar catalyst. Interestingly, this catalyst begins to increase its CO₂ conversion gradually for third testing until achieved maximum conversion of 97.92% at 300 °C. Approximately 100% conversion of CO₂ was obtained over Mn/Ce-75/Al₂O₃ catalyst for fourth testing onwards. Therefore, it can be concluded that the catalyst was
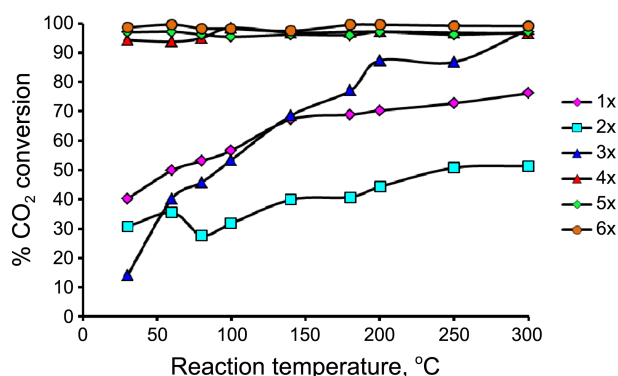
**Figure 12.** Robustness testing at reaction temperature of 100 °C over Mn/Ce-75/Al₂O₃ catalyst calcined at 400 °C for 5 h.

not deactivate even after the sixth testing and can be used for robustness testing.

**Robustness Testing:** The robustness testing towards catalytic activity of Mn/Ce-75/Al₂O₃ (a) was performed on stream continuously for 8 h at reaction temperature of 100 °C. Figure 12 shows the percentage of CO₂ conversion as a function of reaction time over Mn/Ce-75/Al₂O₃ (a).

For the first hour reaction time, the catalyst can convert CO₂ around 96% and maintained above 90% until five hour on stream. The catalyst is then started to deactivate until it reached 7.58% at the end of the test. Therefore, it can be concluded that this catalyst is stable on stream for only 5 h.

## Conclusion

Overall performance from the catalytic activity studies did not yield any catalyst that gives 100% conversion of CO₂ at lower reaction temperature. However, Mn/Ce-75/Al₂O₃ catalyst was assigned as the most potential catalyst for the CO₂ conversion since it gave higher BET surface area with smaller aggregated particle sizes compared to the cerium catalyst promoted by Ni and Cu. This catalyst was prepared using wetness impregnation technique, aging at 85 °C and followed by calcination at 400 °C for 5 h. It can convert CO₂ around 49.05% at 100 °C, 56.79% at 200 °C and maximum CO₂ conversion of 69.44% with 27.35% of methane at reaction temperature of 300 °C. This catalyst can be recycled without deactivation.

**Figure 11.** The trend plot of reproducibility testing over Mn/Ce-75/Al₂O₃ catalyst calcined at 400 °C for 5 h towards CO₂ conversion in methanation reaction.
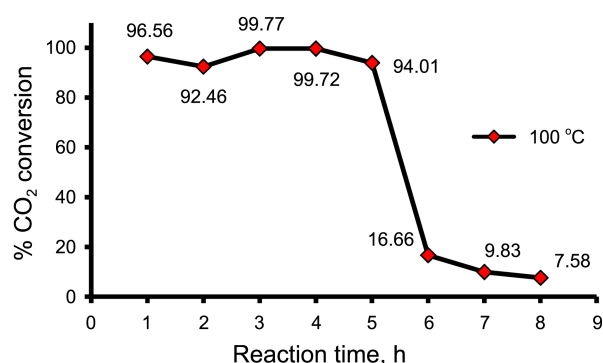
## References

1. Kevin, W. *Human Development Report 2007/2008: Fighting Climate Change, Human Solidarity in a Divided World*; Palgrave Macmillan: New York, 2007; pp 1-399.
2. Haresh, K. *Coal Fired Thermal Power Plant: The Basic Steps and Facts*; Bright Hub Inc: New York, 2010; pp 1-10.
3. Park, N.-K.; Han, D. C.; Han, G. B.; Ryu, S. O.; Lee, T. J.; Yoon, K. J. *Fuel.* **2007**, *86*, 2232-2240.
4. Zhu, T.; Kundakovic, L.; Dreher, A.; Flytzani-Stephanopoulos, M. *Catal Today* **1999**, *50*, 381-397.

5. Nor Aishah, S. A.; Istadi.; Tung, C. Y.; Ruzina, I. *Methane-Carbon Dioxide Conversions to Syngas and Hydrocarbons*; Penerbit UTM Press: Malaysia, 2008; pp 1-9.

6. Rao, G. R.; Mishra, B. G. *Bull. Catal. Soc. India*. **2003**, *2*, 122-134.

7. Hwang, S.; Hong, U. G.; Lee, J.; Baik, J. H.; Koh, D. J.; Lim, H.; Song, I. K. *Catal. Lett*. **2012**, *142*, 860-868.

8. Seo, J. G.; Youn, M. H.; Song, I. K. *J. Power Sources* **2007**, *168*, 251-257.

9. Lee, S. M.; Park, K. H.; Kim, S. S.; Kwon, D. W.; Hong, S. C. *J. Air Waste Manage*. **2012**, *62*, 1085-1092.

10. Peña, D. A.; Uphade, B. S.; Smirniotis, P. G. *J. Catal*. **2004**, *221*, 421-431.

11. Kosmambetova, G. R.; Moroz, E. M.; Guralsky, A. V.; Pakharukova, V. P.; Boronin, A. I.; Ivashchenko, T. S.; Gritsenko, V. I.; Strizhak, P. E. *Int. J. Hydrogen Energ.* **2011**, *36*, 1271-1275.

12. Ocampo, F.; Louis, B.; Kiennemann, A.; Roger, A. C. *Mater. Sci. Eng*. **2011**, *19*, art. no. 012007.

13. Zhang, R.; Li, F.; Shi, Q.; Luo, L. *Appl. Catal. A-Gen.* **2001**, *205*, 279-284.

14. Oh, S. W.; Bang, H. Y.; Bae, Y. C.; Sun, Y. K. *J. Power Sources* **2007**, *173*, 502-509.

15. Perego, C.; Villa, P. *Catal. Today* **1997**, *34*, 281-305.

16. Zou, X.; Wang, X.; Li, L.; Shen, K.; Lu, X.; Ding, W. *Int. J. Hydrogen Energ*. **2010**, *35*, 12191-12200.

17. Perkas, N.; Amirian, G.; Zhong, Z.; Teo, J.; Gofer, Y.; Gedanken, A. *Catal. Lett*. **2009**, *130*, 455-462.

18. Seiyama, T. *Catal. Rev*. **1992**, *34*, 280-300.

19. Kim, S. H.; Nam, S.-W.; Lim, T.-H.; Lee, H.-I. *Appl. Catal. B-Environ*. **2008**, *81*, 97-104.

20. Tada, S.; Kikuchi, R.; Urasaki, K.; Satokawa, S. *Appl. Catal. A-Gen*. **2011**, *404*, 149-154.